CHINESE JOURNAL OF GEOCHEMISTRY: 2006 Vol. 25 No. 4

DOI: 10.1007/s11631-006-0301-y

# Geochronology of a surface core in the northern basin of Lake Qinghai: Evidence from $^{210}$Pb and $^{137}$Cs radionuclides*

XU Hai (徐海)**, AI Li (艾莉), TAN Liangcheng (谭亮成), and AN Zhisheng (安芷生)

*State Key Laboratory of Loess and Quaternary Geology, Institute of Earth Environment, Chinese Academy of Sciences, Xi'an 710075, China*

**Abstract** The radioactivities of $^{210}$Pb and $^{137}$Cs have been measured to estimate the dates of the sediments of a surface core (QH0407-C-2) in the northern basin of Lake Qinghai. The sedimentation rate derived from $^{210}$Pb radioactivity correlates well with that inferred from $^{137}$Cs radioactivity. The dates calculated from depth sedimentation rate (cm/a) are similar to those derived from mass accumulation rate ($g \cdot cm^{-2} \cdot a^{-1}$) between 0－5 cm, but are significantly different below 5 cm, which has been ascribed to the compaction of surface sediments during early diagenesis. The dates derived from mass accumulation rate are consistent with those calculated from the AMS $^{14}$C dating model. The precipitation-controlled indices based on the chronology data derived from mass accumulation rate are similar in trends to the precipitation reconstructed from tree rings in adjacent region, which further verifies the reliability of the geochronology data.

**Key words** $^{210}$Pb; $^{137}$Cs; depth sedimentation rate; mass accumulation rate; Lake Qinghai

## 1 Introduction

The radionuclides $^{210}$Pb and $^{137}$Cs are of particular importance for estimating the dates of recent sediments. It was Goldberg (1963) who firstly suggested that the disequilibrium between $^{210}$Pb and $^{226}$Ra could serve as a geochronometer applicable to recent sediments. Goldberg (1963) successfully attested his hypothesis with a Greenland ice-sheet, which had been previously dated by stratigraphic techniques. Since then, the $^{210}$Pb dating method has found wide applications in determining sedimentation rates for many natural archives such as lake sediments (Krishnaswamy et al., 1971), marine sediments (Koide et al., 1972), and peatland sediments (Pakarinen and Tolonen, 1977). Meanwhile, the atmospheric $^{137}$Cs fallout has been widely used as a time-marker. The $^{137}$Cs fallout increased significantly after 1954 because of nuclear weapon testing, with its highest flux appearing around 1963. Although some $^{137}$Cs peaks around 1974 were reported from some lakes, such as the Hongfeng Lake and the Dianchi Lake in Southwestern China (Wan Guojiang, 1999), and some Chernobyl accident-derived $^{137}$Cs peaks around 1986 were detected from some Europian areas, the highest flux of $^{137}$Cs fallout appeared mainly around 1963 in most parts of the world (He et al., 1996; Robbins et al., 2000; Bergan, 2002; Lu, 2004).

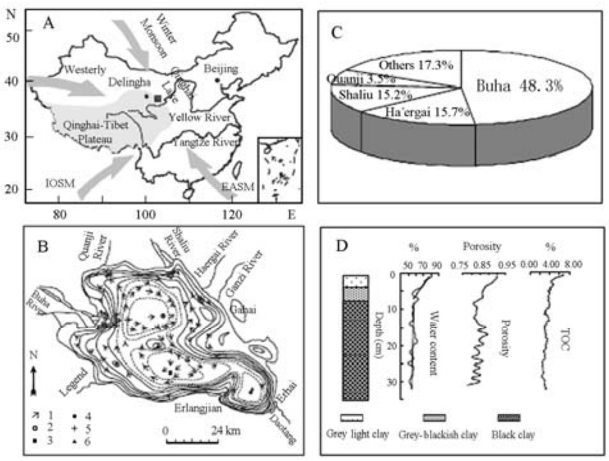


Fig.1 A. Location of Lake Qinghai (solid rectangle). ISM and EASM denote the Indian Summer Monsoon and the East Asian Summer Monsoon, respectively. B. Locations of core QH0407-C-2 in the northern basin (this study), core QING6 in the southern basin (Henderson et al., 2003), and core QH00A and core QH2000 in the southeastern basin (Shen Ji et al., 2001; Liu et al., 2002). 1. Surface lake current; 2. location of QH0407-C-2; 3. location QING6; 4. location of QH00A; 5. location of QH2000; 6. Haixin Mountain. C. Percentage of the inflowing water volume of each river compared to the total volume of the inflowing surface water. D. Lithology, water content, porosity and total organic carbon of the surface sediments of core QH0407-C-2.

ISSN 1000-9426

* This work is supported by the National Basic Research Program of China (No.2004CB720207), and by the National Natural Science Foundation of China (No.40599422).

*Corresponding author, E-mail: xuhai2003@263.net

Lake Qinghai, the largest closed semi-saline inland lake in China, is located in the northeastern part of the Qinghai-Tibet plateau, where the Indian summer monsoon, the East Asian summer monsoon, winter monsoon, and the westerly prevail (Fig.1A). About a quarter of the total population and 29% of the livestock in Qinghai Province are supported by the lake and surrounding vegetations. The scientific and economic significance of Lake Qinghai has long been recognized world wide. Accurate dates of the surface sediments are crucial to understand the sediment-tary/geochemical processes, and to evaluate and predict the sustainability of Lake Qinghai. Up to now, only a few surface cores in Lake Qinghai, such as core QING6 in the southern basin (Henderson et al., 2003) and core QH00A in the southeastern basin (Shen Ji et al., 2001), have been reported to be dated by the $^{210}$Pb and $^{137}$Cs methods (Fig.1B). However, the previous $^{210}$Pb/$^{137}$Cs-dates, which had been calculated in terms of depth sedimentation rates (e.g. cm/a), may have seriously suffered from the compaction of sediments during early diagenesis. Efforts to understand the effects of compaction on the surface sediments are necessary to acquire reliable chronology data for the surface sediments of Lake Qinghai.

In this study the $^{210}$Pb and $^{137}$Cs dating methods were employed to determine the dates of sediments in a surface core in the northern basin of Lake Qinghai. It was found that the chronology data calculated in terms of mass accumulation rates are significantly different from those calculated in terms of depth sedimentation rates. The chronology data obtained on the basis of mass accumulation rates have been verified both by the AMS $^{14}$C dating model and by comparisons with the dendrochr-onology data reported from adjacent region (see below).

## 2 Background, sampling and method

Lake Qinghai (36°32′−37°15′N, 99°36′−100°47′E; Fig.1), formed in the process of neotectonic uplifting of the Qinghai-Tibet plateau, lies in an intermountain basin and is now hydrologically closed. The surface area of the lake is about 4400 km$^2$ and the catchment area is about 29660 km$^2$ (LZBCAS, 1994). Bedrocks of the catchment area consist of sedimentary rocks (e.g. shale and sandstone), metamorphic rocks (e.g. gneiss and schist) and a small fraction of igneous rocks (e.g. granite). Seven large rivers flow into the lake (Fig.1B). The inflow water volume of the four main rivers in the northern and northwestern catchment areas, namely the Buha River, the Quanji River, the Shaliu River and the Ha'ergai River, accounts for more than 80% of the total volume of the inflow surface water (Fig.1C).

Surface sediments were collected undistubedly with a self-designed gravity corer, then sealed and preserved *in-situ* in ice-box. Remarkable litho-stratigraphic differences exist between the upper parts of all the cores and the deeper layers. Sediments from the upper 7-cm depth are grey clay, of which the uppermost 3 cm is light grey and the underlying 4 cm is grey-blackish. Sediments at the lower 7-cm depth are blackish clay (Fig.1D).

Core QH0407-C-2, 33 cm long (100°18.176′E, 37°03.476′N, water depth: 22.0 m), was cut into slices measured at 1 cm in thickness. Wet mass of each sample was measured immediately. Sediments were dehydrated by means of centrifugation (3500 rpm, 4℃, 20 min) and then freeze-dried. Water contents of the sediments were calculated based on the mass of dry and wet samples. Porosity of the sediments was calculated using the following equation:

$$\phi = 1 - \frac{W_{dry}}{\rho_{solid} \times V} \qquad (1)$$

where $\phi$ is the porosity, $W_{dry}$ is the mass of dry sample, V is the wet volume of each sample, $\rho_{solid}$ is the density of the solid (about 2.5 g/cm$^3$ in general).

Mass depth ($Z$) of section $i$ is calculated from the following equation:

$$Z_i = \sum (1-\phi_i) \times \rho_{solid} \times X_i \qquad (2)$$

where $\phi_i$ and $X_i$ are the porosity and depth of section $i$, respectively.

Dry samples were grounded as fine as to be 150 mesh. The activities of $^{210}$Pb and $^{137}$Cs were measured by multi-channel gamma-ray spectrometry (Canberra, S-100), with a reverse-electrode (REGe) and XtRa detector (Bai et al., 2002). $^{137}$Cs activity was measured at 661.6 keV, while $^{210}$Pb at 46.5 keV. The relative detect efficiency is 30%. The experimental error is less than 10%.

## 3 Results

The activities of $^{210}$Pb below the 9-cm layer are relatively constant, with an average of 0.05 Bq/g (Fig.2A), which can be approximately regarded as the supported $^{210}$Pb. The excess $^{210}$Pb can be estimated using the total $^{210}$Pb activity to minus the supported $^{210}$Pb activity. The $^{210}$Pb$_{ex}$ at the lower 9-cm depth is assumed to be zero because variations in $^{210}$Pb$_{ex}$ at the lower 9-cm depth are very small and should be logically non-negative (Fig. 2A).

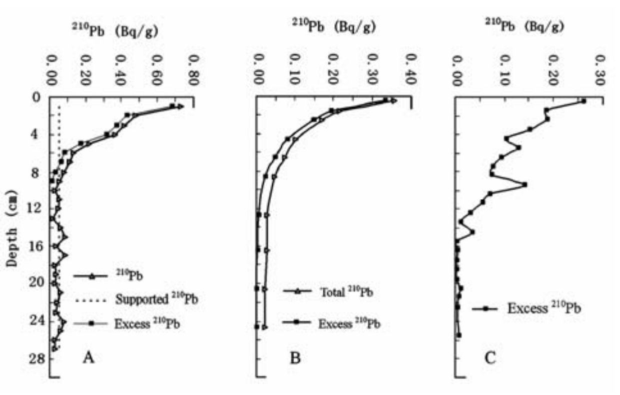


Fig. 2. Radioactivities of $^{210}$Pb in core QH0407-C-2 (A), core QING6 (B) (from Henderson et al., 2003), and core QH00A (C) (from Shen Ji et al., 2001).

The concentrations of $^{210}Pb_{ex}$ in the upmost 1-cm-section of core QH0407-C-2 (about 0.68 Bq/g; Fig.2A) are much higher than those of core QING6 in the southern basin (about 0.35 Bq/g; Fig.2B; Henderson et al., 2003) and those of core QH00A in the southeastern basin (about 0.26 Bq/g; Fig.2C; Shen Ji et al., 2001). The $^{137}$Cs flux of core QH0407-C-2 is also much higher than that of core QH00A (Fig.3). As mentioned above, the inflow water volume of the four main rivers in the northern and northwestern catchment areas accounts for more than 80% of the total volume of surface inflow water (Fig.1C). Therefore, more $^{226}$Ra and atmospherically deposited nuclides would be brought into the northern basin. Moreover, currents in the lake pass through the northern basin prior to the other two basins (Fig.1B), which would lead to a stronger scavenging of the nuclides from the water column in the northern basin than in other places. The Daotang River in the southeastern catchment area flows into the Erhai Lake prior to the southeastern basin, which will prevent the nuclides from entering the southeastern basin directly (Fig.1B). Therefore, the surface concentrations of nuclides in the southeastern basin are lowest relative to those in the northern and southern basins, respectively (Figs.2 and 3). Such a process-dependent distribution of nuclides has been reported in numerous studies. For example, in the East China Sea, the inventories of $^{137}$Cs and $^{210}$Pb tend to decrease away from the estuarine sources (Huh and Su, 1999). The inventory of $^{137}$Cs in South Baikal near the Selenga River is about 6-10 times higher than in North Baikal, which is probably due to the input of the Selenga River in the southern region that extends to a wide region in Mongolia, as suggested by Carroll et al. (1999). The inventory of $^{137}$Cs near the river mouth of the Ise Bay, Japan, is also much higher than in other places (Lu and Matsumoto, 2005). Even in a small lake like Lake Saltonstall in eastern USA (Benoit and Rozan, 2001), there exist significant differences in total inventory of both $^{210}$Pb and trace metals between the cores examined recently and those studied in the past.

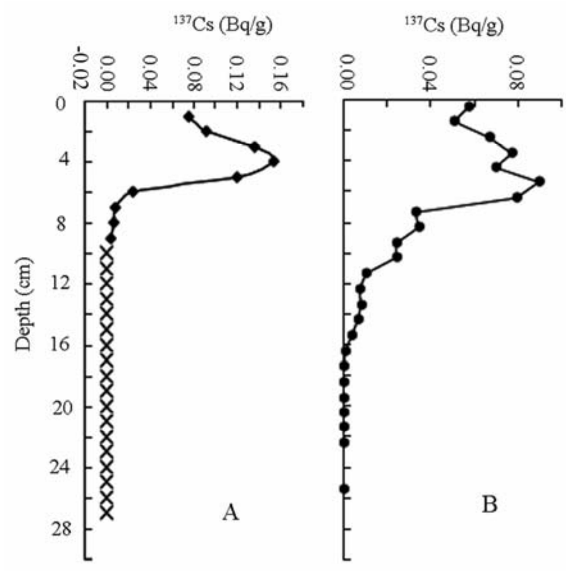


Fig. 3. Radioactivities of $^{137}$Cs in core QH0407-C-2 (A) and core QH00A (B) (from Shen Ji et al., 2001). "×" denotes the radioactivity lower than the detectable limit.

## 4 Discussion

### 4.1 $^{210}$Pb dates

The bio-disturbance of sediments and disturbance in response to the precipitation processes may more or less influence the dating results. Therefore, it is reasonable to use the fits of $^{210}Pb_{ex}$ to estimate sedimentation rates (Fig.4). Moreover, since the total $^{210}$Pb activities in the 8-cm- and 9-cm-sections are very close to those of the supported $^{210}$Pb (Fig.2), we used the data from the upper 8-cm-section to estimate the dates of the surface sediments.

$^{210}Pb_{ex}$ decreases downwards exponentially (Fig.4A). The fitted curve intersects with the $^{210}Pb_{ex}$ at about 0.95 (Bq/g) at 0 cm (or 0 g•cm$^{-2}$), suggesting that the initial $^{210}Pb_{ex}$ concentration ($C_0$) is approximately 0.95 Bq/g. The significantly linear relationship between Ln ($^{210}Pb_{ex}$) and mass depth (Fig.4B) suggests that the flux of $^{210}Pb_{ex}$ (F), the sedimentation rate (S) and F/S (or $C_0$) should be relatively constant. Therefore, we applied the CFCS, CIC, and CRS models to estimate the $^{210}$Pb dates (Refer to Heyvaert (1998) for details of the models).

The CIC, CFCS, and CRS models give similar ages (Fig.5A, B). The CRS age is slightly younger than both CIC age and CFCS age at the upper

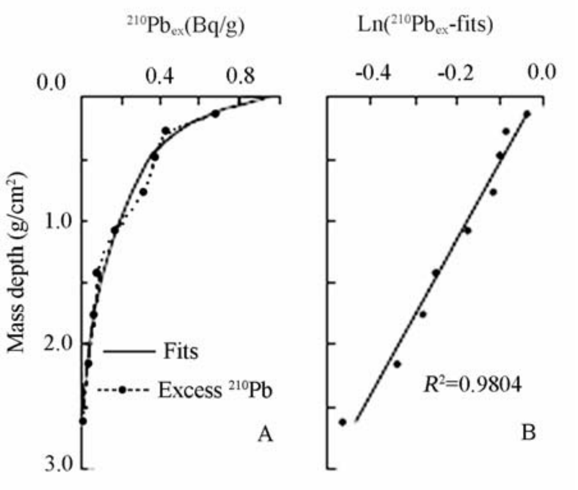


Fig. 4. The excess $^{210}$Pb and logarithm-fits (A). Linear correlation between the logarithm of the fits and mass depth (B).

4-cm-section, while the CRS age is slightly older than the CIC age and CFCS age 4-cm-section below (Fig.5A). When sedimentation rate increases systematically, the initial concentrations ($C_0$) will decrease since the supply of $^{210}Pb_{ex}$ keeps relatively constant. Under this circumstance, the CIC model will give older ages because $C_0$ used in the model is higher than its true value. On the contrary, when sedimentation rate decreases, the CIC model will give ages younger than the true values. Therefore, when

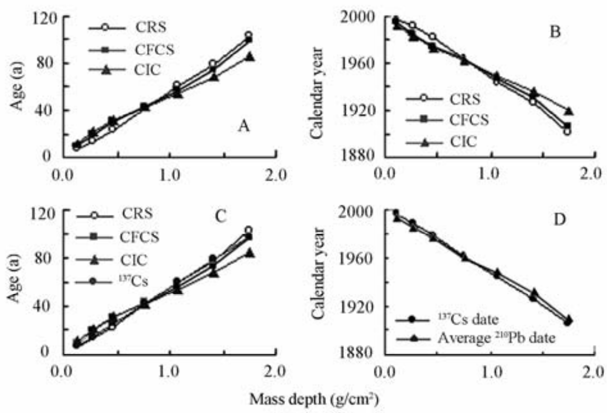


Fig. 5. $^{210}$Pb ages (A) and related dates (B) derived from CRS, CFCS, and CIC models. The $^{137}$Cs time marker gives similar ages to those derived from $^{210}Pb_{ex}$ (C). The average of the CRS-, CFCS-, and CIC-dates correlates much better with the $^{137}$Cs-dates (D).

sedimentation rate increases, the sedi- mentation rate calculated by CRS will be higher than that calculated by CIC; when sedimentation rate decreases, the sedimentation rate calculated by CRS will be lower than that calculated by CIC. The younger CRS ages (Fig.5A) after 1963 (the upmost 4-cm section) possibly indicate a systematic increase in sedimentation rate; while the older CRS-ages before 1963 (the 4 cm below) possibly indicate a systematic decrease in sedimentation rate. This seems to be a reasonable explanation because of the increases of biomass, chemical deposition, and inflowing materials due to the warming trend around Lake Qinghai during the past 40 years.

Differences between CIC-, CFCS- and CRS-ages become more distinct with increasing depth. The difference between CIC- and CRS-ages is 10 years for the 6-cm-section and is 18 years for the 7-cm-section (Fig.5A), which will lead to quite different sedimentation rates. Therefore, dates of the sediments below the 5-cm depth should be more reliable to be extrapolated from an average sedimentation rate (see below).

## 4.2 $^{137}$Cs dates

It is difficult to evaluate the reliability of the dates inferred merely from a single radionuclide. The $^{210}$Pb geochronology data should be validated using at least one independent time-marker. Since no varve has been discovered in the surface sediments of Lake Qinghai, the $^{137}$Cs time-marker is critical to verify the $^{210}$Pb ages. As mentioned above, the highest atmospheric $^{137}$Cs peaks are around 1963 in general. Although some bio-disturbance and vertical redistribution of $^{137}$Cs will influence the shape of the $^{137}$Cs peak, the horizontal position of the $^{137}$Cs peak will not change, which ensures the reliability of the $^{137}$Cs peak as a time marker. The $^{137}$Cs peak of 1963 is produced in the 4-cm-section in core QH0407-C-2. Depth sedimentation rate based on this peak is about 0.10 cm/a, and mass accumulation rate is about 0.018 $g \cdot cm^{-2} \cdot a^{-1}$.

The $^{137}$Cs dates correlate well with the $^{210}$Pb dates, especially at the 4-cm-section where the $^{137}$Cs date is 1963, while the CRS date is 1963, the CIC date is 1962, and the CFCS date is 1962 (Fig.5C). The $^{137}$Cs dates correlate much better with the average of the dates derived from different $^{210}$Pb models (Fig.5D). Average mass accumulation rate is about 0.018 $g \cdot cm^{-2} \cdot a^{-1}$ inferred from the $^{137}$Cs dates and from the average $^{210}$Pb dates, which will be used to extrapolate the dates of the sediments below the 5-cm depth (see below).

## 4.3 Differences between the dates calculated from depth sedimentation rate and mass accumulation rate for core QH0407-C-2

As shown in Fig.6, the dates derived from depth sedimentation rate are similar to those derived from mass accumulation rate at the upper 5-cm depth, but are quite different at the lower 5-cm depth. The differences tend to become more significant with increasing depth. Date of the 27-cm-section (the lowermost section measured in this study) is 1734 estimated from an average depth sedimentation rate (0.10 cm/a), but is 1464 inferred from an average mass accumulation rate (0.018 $g \cdot cm^{-2} \cdot a^{-1}$). Such a big difference will give rise to big uncertainties for accuracy dates. Lithology, water content, porosity,

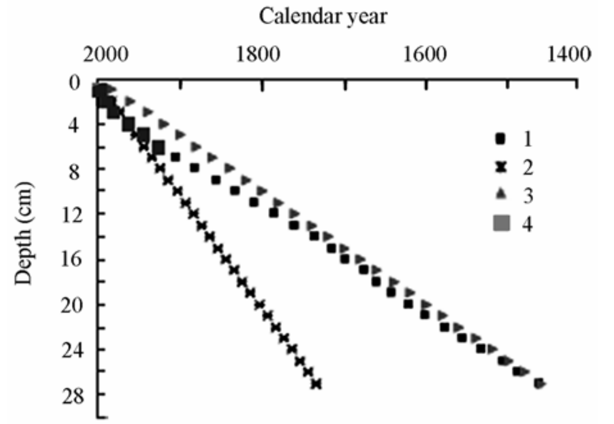


Fig. 6. Dates of the sediments derived from mass accumulation rate (small solid rectangle), from depth sedimentation rate (asterisk), and from the AMS $^{14}C$ dating frame (blackish solid triangle). The solid rectangle (bigger) denotes the average of the $^{210}Pb$ dates and $^{137}Cs$ dates calculated directly from the measured $^{210}Pb$ and $^{137}Cs$ radioactivities. 1. Date derived from mass accumulation rate; 2. date derived from depth sedimentation rate; 3. date derived from AMS $^{14}C$ dating frame; 4. average dates calculated from the measured $^{210}Pb$ and $^{137}Cs$.

and total organic carbon (Fig.1D) of the surface sediments show significant differences between the upper 7-cm and the lower 7-cm depth, indicating obviously early diagenesis. Because of the compaction of lake sediments during early diagenesis, dates of the sediments at the lower 7-cm depth are theoretically unsuitable to be extrapolated using the depth sedimentation rate calculated from the dates of the sediments at the upper 7-cm depth. However, the compaction of the sediments will not theoretically influence the dates calculated from mass accumulation rate (Wan Guojiang, 1999). Therefore, dates derived from the mass accumulation rate are expected to be reliable.

## 4.4 Test of the geochronology data of core QH0407-C-2

Depth sedimentation rate between 0−4 cm depths below the surface is about 0.10 cm/a, which is similar to that of core QING6 in the southern basin (about 0.10 cm/a; Henderson et al., 2003) and is slightly lower than that of core QH00A in the southeast basin (about 0.12 cm/a; Shen Ji et al., 2001). The vertical distribution characteristics of proxy indices such as total organic carbon (TOC), total carbonate content, grain size and geomagnetism, are similar among the three basins for surface sediments (Zhang et al., 2003), suggesting similar sedimentation rates for these three deepest basins. Therefore, the dates of surface sediments at the same depth should be similar for these three deepest basins.

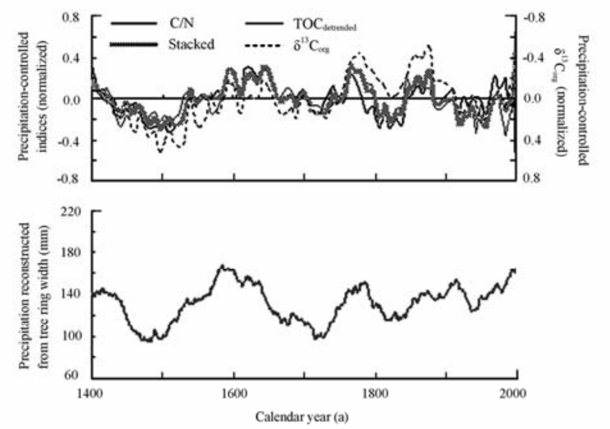


Fig. 7. Precipitation-controlled indices for the surface sediments of Lake Qinghai (unpublished data) based on the dates calculated from mass accumulation rate (upper panel) and precipitation reconstructed from tree-ring width index (31-year running mean) in Delingha (lower panel; Shao et al., 2005). The indices plotted in the upper panel are normalized and the stacked curve represents the average of the normalized C/N, TOC, and $\delta^{13}C_{org}$ values.

As revealed from previous studies, the AMS $^{14}C$ age is about 2400±100 a BP at the 120-cm depth for core QH2000 (see Fig.1B) in the southeast basin (Liu et al., 2002). Given a similar sedimentation rate in the north basin, dates of the sediments of core QH0407-C-2 can be estimated (Fig.6). The dates estimated from the AMS $^{14}C$ data are much closer to those derived from mass accumulation rate, suggesting that the mass accumulation rate is more reliable to estimate the dates of surface sediments of Lake Qinghai.

$\delta^{13}C$ and C/N values of organic matter, and total organic carbon in the surface sediments of core QH0407-C-1 (collected at the same site as QH0407-C-2), were suggested to be controlled predominantly by precipitation (unpublished data). As shown in Fig.7, the precipitation-controlled indices based on the dates calculated from the mass accumulation rate are similar in trends to the precipitation reconstructed from tree-ring widths in Delingha (see location in Fig.1A) near Lake Qinghai (Shao et al., 2005), which further confirms the dates based on mass accumulation rate.

## 5 Summary

The radioactivities of $^{210}$Pb and $^{137}$Cs in the sediments of a surface core (QH0407-C-2) in the northern basin of Lake Qinghai have been measured to estimate the dates of the surface sediments. Sedimentation rates derived from $^{210}$Pb radioactivity correlates quite well with that inferred from $^{137}$Cs radioactivity.

The lithology, water content and TOC of the sediments show remarkable differences between sediments at the upper 7-cm and the lower 7-cm depths, which should be ascribed to the early diagenesis of the sediments. The compaction of the surface sediments during early diagenesis leads to remarkable differences between the dates calculated from depth sedimentation rate (cm/a) and those derived from mass accumulation rate ($g \cdot cm^{-2} \cdot a^{-1}$). Dates of the sediments at the lower 7-cm depth are theoretically unsuitable to be extrapolated using the depth sedimentation rate derived from the dates of the sediments at the upper 7-cm depth.

The dates derived from mass accumulation rate are consistent with those calculated from the AMS $^{14}$C dating models. The precipitation-controlled indices for the surface sediments of Lake Qinghai based on the chronology data derived from mass accumulation rate are similar in trends with the precipitation inferred from tree rings in adjacent region, which further verifies the reliability of the geochronology data acquired.

## References

Bai Z.G., Wan G.J., Huang R.G., and Liu T.S. (2002) A comparison on the accumulation characteristics of $^{7}$Be and $^{137}$Cs in lake sediments and surface soils in western Yunnan and central Guizhou, China [J]. *Catena*. **49**, 253—270.

Bergan T.D. (2002) Radioactive fallout in Norway from atmospheric nuclear weapons tests [J]. *Environmental Radioactivity*. **60**, 189—208.

Benoit G.and Rozan T.F. (2001) $^{210}$Pb and $^{137}$Cs dating methods in lakes: A retrospective study [J]. *Journal of Palaeolimnology*. **25,** 455—465.

Carroll J., Williamson M., Lerche I., Karabanov E., and Williams D.F.(1999) Geochronology of Lake Baikal from $^{210}$Pb and $^{137}$Cs radioisotopes [J]. *Applied Radiation and Isotopes*. **50**, 1105—1119.

Goldberg E.D. (1963) Geochronology with lead 210. In *Radioactive Dating* [M]. pp. 121—131. IAEA, Vienna.

He Q., Walling D.E., and Owens P.N. (1996) Interpreting the $^{137}$Cs profiles observed in several small lakes and reservoirs in southern England [J]. *Chemical Geology*. **129**, 115—131.

Henderson A.C.G., Holmes J.A., Zhang J.W., Leng M.J., and Carvalho L.R. (2003) A carbon- and oxygen-isotope record of recent environmental change from Lake Qinghai, NE Tibetan Plateau [J]. *Chinese Science Bulletin*. **48**, 1463—1468.

Heyvaert A.C. (1998) *The Biogeochemistry and Palaeolimnology of Sediments from Lake Tahoe, California-Nevada* [D]. Dissertation for Ph.D. University of California.

Huh C. and Su C. (1999) Sedimentation dynamics in the East China Sea elucidated from $^{210}$Pb, $^{137}$Cs and $^{239, 240}$Pu [J]. *Marine Geology*. **160**, 183—196.

Koide M., Soutar A., and Goldberg E.D. (1972) Marine geochronology with $^{210}$Pb [J]. *Earth and Planetary Science Letters.* **14**, 442—446.

Krishnaswamy S., Lal D., Martin J.M., and Meybeck M. (1971) Geochronology of lake sediments [J]. *Earth and Planetary Science Letters*. **11**, 407—414.

LZBCAS (Lanzhou Branch of Chinese Academy of Sciences) (1994) *Evolution of Recent Environment in Qinghai Lake and Its Prediction* [M]. West Center of Resource and Environment, Chinese Academy of Sciences, Science Press, Beijing (in Chinese).

Liu X.Q., Shen J., Wang S.M., Yang X.D., Tong G.B., and Zhang E.L. (2002) A 16000-year pollen record of Qinghai Lake and its paleoclimate and Paleoenvironment [J]. *Chinese Science Bulletin.* **47**, 1931—1937.

Lu X. (2004) Application of the Weibull extrapolation to $^{137}$Cs geochronology in Tokyo Bay and Ise Bay, Japan [J]. *Journal of Environmental Radioactivity*. **73**, 169—181.

Lu X.X. and Matsumoto E. (2005) Recent sedimentation rates derived from $^{210}$Pb and $^{137}$Cs methods in Ise Bay, Japan [J]. *Estuarine, Coastal and Shelf Science*. ***65***, 83—93.

Pakarinen P. and Tolonen K. (1977) On the growth-rate and dating of surface peat [J]. *Finnish Peatland Society.* ***28***, 19—24.

Robbins J.A., Holmes C., Halley R., Bothner M., Shinn E., Graney J., Keeler G., tenBrink M., Orlandini K.A., and Rudnick D. (2000) Time-averaged fluxes of lead and fallout radionuclides to sediments in Florida Bay [J]. *Journal of Geophysical Research.* **105** (C12), 28805—28821.

Shao X.M, Huang L, Liu H.B., Liang E.Y., Fang X.Q., and Wang L.L. (2005) Reconstruction of precipitation variation from tree rings in recent 1000 years in Delingha [J], *Qinghai. Science in China* (D). **48**, 939—949.

Shen Ji., Zhang Enlou, and Xia Weilan (2001) Records from lake sediments of Lake Qinghai to mirror climatic and environmental changes of the past about 1000 years [J]. *Quaternary Sciences.* **21**, 508—513 (in Chinese with English abstract).

Wan Guojiang (1999) $^{137}$Cs dating by annual distinguish for recent sedimentation: Samples from Erhai Lake and Hongfeng Lake [J]. *Quaternary Sciences*. **19**, 72—80 (in Chinese with English abstract).

Zhang J.W., Jin M., Chen F.H., Battarbee R.W., and Henderson A.C.G. (2003) High-resolution precipitation variations in the Northeast Tibet Plateau over the last 800 years documented by sediment cores of Qinghai Lake [J]. *Chinese Science Bulletin*. **48**, 1451—1456.